Radiofrequency Coils and Pulse Sequences for Cardiac Magnetic Resonance Applications: New Perspectives and Future Developments

Giulio Giovannetti, PhD,[1,2] Daniele De Marchi, RT,[2] Alessandro Pingitore, MD, PhD[1]
[1]Institute of Clinical Physiology, National Council of Research, Pisa, Italy; [2]Fondazione G. Monasterio CNR-Regione Toscana, Pisa, Italy

Cardiac magnetic resonance (CMR) is a relevant diagnostic tool for the evaluation of cardiac morphology, function, and mass. The assessment of myocardial tissue content through the measurement of longitudinal (T1) and transversal (T2) relaxation properties and the development of different technical advances are important clinical novelties of CMR. Recently, magnetic resonance spectroscopy has been explored for the assessment of the metabolic state of tissue for cardiac function evaluation by using nuclei other than protons, such as ^{13}C and ^{23}Na, expanding our knowledge of the kinetics of metabolic processes. The design and development of dedicated radiofrequency coils and pulse sequences are fundamental to maximizing signal-to-noise ratio data while achieving faster cardiac examination. This review highlights the new technical developments in CMR sequences and coils.

[Rev Cardiovasc Med. *2016;17(3/4):124-130 doi: 10.3909/ricm0846*]

KEY WORDS

Radiofrequency coils • Pulse sequences • Cardiac magnetic resonance

Cardiac magnetic resonance (CMR) is a relevant diagnostic tool for the evaluation of cardiac disease due to its noninvasive nature, the absence of ionizing radiation, the three-dimensional visualization of the heart chambers, high image quality, and good temporal resolution. Moreover, this rapid clinical expansion is also linked to the potential to assess, in a "one-stop shop" modality, several cardiac characteristics, including regional and global systolic function, morphology, volume chambers, mass and wall thickness, and tissue characterization. Among these diagnostic opportunities, tissue characterization has had a relevant impact on routine clinical practice, allowing clinicians to accurately diagnose infiltrative adipose

tissue within the myocardium (as in patients with arrhythmogenic right ventricular cardiomyopathy), the presence of myocardial edema (as in patients with acute myocarditis), and the presence of severe myocardial damage (such as no-reflow in acute myocardial infarction).

Although this is the current state of the art of CMR in the clinical arena, magnetic resonance spectroscopy (MRS) represents its near-future development. This technique allows selective identification of molecules and molecular distribution mapping within various organs, and is a powerful tool to explore the tissue components and myocardium metabolism. MRS uses the signal from a range of nuclei, including ^{31}P, ^{1}H, ^{13}C, and ^{23}Na, to expand our knowledge of the kinetics of metabolic processes and their role in myocardial disease. Nevertheless, a number of technologic problems still limit this technology and require innovative solutions. When a clinical scanner must be used, the design and the development of dedicated radiofrequency (RF) coils and the use of novel pulse sequences[1] are required for the successful realization of CMR experiments. This review highlights the new technical developments in CMR sequences and coils. The development of these elements is fundamental for obtaining faster cardiac examination with the same image quality, for increasing the diagnostic potential of this technique to detect diseases at earlier and more reversible phases of evolution, and for better stratification of the severity of disease (and thus prognosis of patients).

Hardware

The key components in magnetic resonance systems include a main magnet, a set of gradient coils, and RF coils. The purpose of the transmitter coil is to produce a highly homogeneous alternating field in a wide field of view because the extension of the region under analysis is not known a priori. Therefore, transmit coils are usually large to optimize field homogeneity and include a significant volume of tissue. The function of the receiver coil is to maximize signal detection while minimizing noise; for this purpose, it is optimal to minimize the coil dimensions.[2] Many different coils have been designed[3] and, according to their shapes, they can be categorized into volume coils and surface coils. The first group can be used both for transmission and reception; birdcage coils are popular due to their ability to generate a highly homogenous RF magnetic field with a high signal-to-noise ratio (SNR).

Phased-array coils also allow for the implementation of parallel imaging, which is a technique that may provide substantial reductions in image acquisition time.

Surface coils, composed of loop coils of various shapes, are usually much smaller than volume coils and, therefore, have a higher SNR because they receive noise only from nearby regions. However, they have a relatively poor field homogeneity and are therefore mainly used as receive coils.

The ideal setup should comprise the use of two different coils: a transmit coil, made up of a homogeneous volume resonator for achieving an efficient excitation in a large volume, and a receive coil, characterized by a high local sensitivity. The use of phased-array coils[4] provides a larger sensitivity region, similar to that obtained with volume coils, and a high SNR, usually associated with surface coils. Phased-array coils also allow for the implementation of parallel imaging,[5] which is a technique that may provide substantial reductions in image acquisition time.

Figure 1 shows examples of different geometry coils. In particular, Figure 1A and Figure 1B show, respectively, a surface coil and a quadrature birdcage coil, both designed for cardiac metabolism assessment in pig models. Figure 1C shows a commercial four-element array coil for cardiac studies.

Coils have to be optimized for application in CMR. For example, the use of a cardiac surface coil provides a higher SNR but can be problematic; inferolateral regions may have a lower signal intensity due to the longer distance to the coil plane and thus should only be used if an efficient coil intensity correction algorithm is implemented.[6]

… birdcage coils are popular due to their ability to generate a highly homogenous RF magnetic field with a high signal-to-noise ratio.

Since the development of phased-array coils, magnetic resonance vendors introduced multiple receiver channel systems to take advantage of the improved sensitivity and extended field of view provided by the multiple coil design.[7] Currently, CMR systems use at least 8-channel devices and are often equipped to expand to 16 channels. Recently, the implementation of parallel imaging techniques in combination with dedicated 32-channel coil arrays significantly shortened data acquisition time in cardiovascular imaging.[5]

Software in the Clinical Application

Established Techniques

Spin echo sequences are used for anatomic imaging and tissue

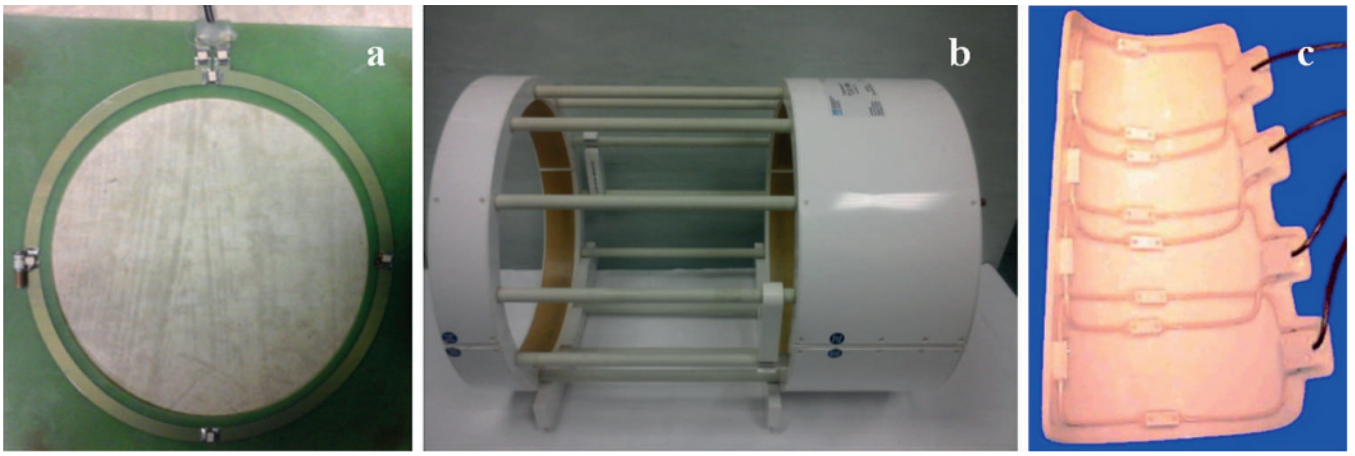

Figure 1. Images of different radiofrequency coils. **(A)** surface; **(B)** volume; **(C)** phased-array.

characterization, whereas gradient echo sequences are used for acquiring cine images to calculate volumes and to assess regional and global cardiac function in both right and left ventricles. These sequences are commonly used in daily clinical practice to detect fibrosis, edema, fat, hemorrhage, or infiltrative diseases within the myocardium as a consequence of acute or chronic cardiac diseases. In particular, fast spin echo T1- or proton density-weighted sequences (Figure 2) are used to detect fat infiltration within the myocardium.

In the fast spin echo T2-weighted or inversion recovery (fat saturation) sequences (Figure 3), water has higher signal intensity than myocardium, and is used to detect myocardial edema caused by inflammation or acute ischemia.[8]

Furthermore, fat suppression is used to increase contrast between water and myocardial tissue. It consists of applying an additional 180° pulse after an inversion time settled to match the null time of fat. This technique depends on the fat T1, which is shorter than that of most other tissues, and is performed by using a short T1 inversion recovery sequence.[9] T1-weighted sequences are largely employed for obtaining images with the late gadolinium enhancement technique (Figure 4).[10]

In particular, the inversion-recovery gradient-echo sequence provides high contrast between normal myocardium and scarring by nulling the signal from normal myocardium. This sequence is largely used in the clinical setting to assess the presence of fibrosis within the myocardium, which is the final common way of differentiating between cardiac diseases, including the ischemic and nonischemic ones (such as idiopathic dilated or hypertrophic cardiomyopathy), and the infiltrative ones (such as amyloidosis and sarcoidosis).[11] The myocardial late gadolinium enhancement study, based on T1-weighted ultrafast gradient echo or steady-state gradient echo sequences, is performed approximately 10 minutes after contrast agent injection and

Figure 2. Fast spin echo proton density-weighted image. This image was acquired by using a 1.5T scanner (Signa Excite General Electric, Waukesha, WI). Informed consent was obtained for experimentation with a human subject.

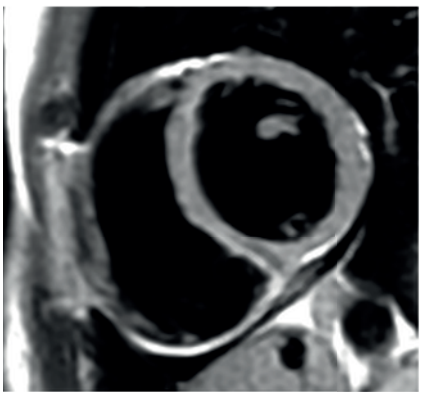

Figure 3. Inversion-recovery fast spin echo image. This image was acquired by using a 1.5T scanner (Signa Excite General Electric, Waukesha, WI). Informed consent was obtained for experimentation with a human subject.

Figure 4. Steady-state free-precession image.

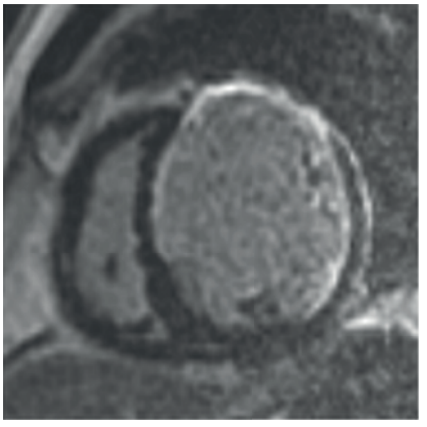

transmits a relative excess of gadolinium in the pathologic tissues compared with healthy tissues. In addition to T1 and T2 imaging, T2* imaging permits noninvasive detection of myocardial iron deposition.[12] T2*-weighted sequences are sensitive to the degradation of hemoglobin products, and are used for hemorrhage detection.[13] The T2* magnetic resonance imaging (MRI) technique is the gold standard for myocardial iron characterization and has opened up the opportunity to investigate myocardial iron overload in transfusion-dependent adults in a noninvasive and reliable way.[14] Cine imaging is performed in planes oriented to the shape of the heart, including two-chamber, four-chamber, and short-axis views. The functional information derived by cine CMR includes global left and right ventricular volumes and mass, and the most basic cine technique employs a gradient echo sequence synchronized to the patient ECG. Recently, steady-state free-precession (SSFP) has become the standard sequence for cardiac function imaging, due to its potential to provide high contrast between chamber blood (white) and myocardium (dark).[15] The basic principle of SSFP is based on the application of a fast train of pulses interleaved by periods of so-called "free precession," characterized by the absence of excitation. Depending on the different gradient switching patterns applied within the free precession period or the pulse phase changes, different steady states are established.[16] Although other pulse sequences permit the production of "movies" of the cardiac cycle, SSFP is characterized by a high degree of spatial and temporal resolution, because an entire stack of short-axis images can be acquired within a single breath-hold (Figure 5).[17]

Cine imaging is performed in planes oriented to the shape of the heart, including two-chamber, four-chamber, and short-axis views.

Myocardial perfusion imaging can be performed by contrast-enhanced first-pass imaging, which consists of using inversion-recovery gradient-echo imaging after injection of a bolus of gadolinium-diethylenetriamine penta-acetic acid for observing first contrast agent transit through the cardiac chambers and myocardium.[18] This technique is largely used in the clinical setting for the assessment of myocardial ischemia through pharmacologic stress tests.

Different and important cardiac functions can be studied with blood oxygen level-dependent (BOLD) CMR, which directly reflects myocardial oxygenation status. It is based on the paramagnetic properties of deoxyhemoglobin as an endogenous contrast agent, with increased deoxyhemoglobin content leading to signal reduction on T2*- or T2-weighted images.[19] BOLD has been recently used for detecting stress-inducible myocardial ischemic reactions in the presence of angiographically significant coronary artery disease.[20]

BOLD has been recently used for detecting stress-inducible myocardial ischemic reactions in the presence of angiographically significant coronary artery disease.

The implementation of parallel imaging techniques in combination with dedicated multi-element coil arrays significantly shortens data acquisition time in CMR. At the same time, MRI sequences have been optimized to exploit array coils for spatial encoding, as in sensitivity encoding,[21] simultaneous acquisition at spatial harmonies,[22] and generalized autocalibrating partially parallel acquisitions.[23] More recently, various other techniques have been developed for reducing acquisition times, such as sensitivity profiles from an array of coils for encoding and reconstruction in parallel,[24] parallel magnetic resonance imaging with adaptive radius in k-space,[25] and iterative self-consistent parallel imaging reconstruction.[26]

Figure 5. Late gadolinium-enhanced image.

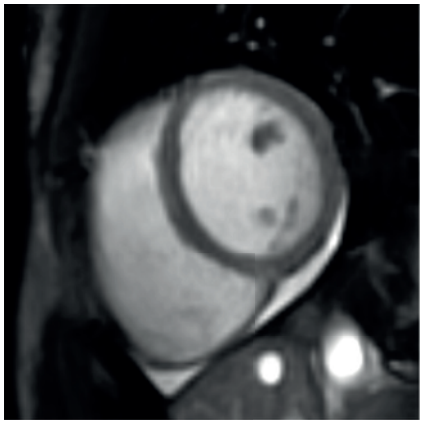

Newly Described Techniques

Tissue characterization through assessing myocardial T1 and T2 mapping and spectroscopy currently represent the two primary fields of CMR development. The measurement of T1 and T2 mapping aims to detect early myocardial degenerative and infiltrative diseases, whereas spectroscopy aims to assess myocardial metabolism. In general, accurate T1 estimation is achieved from a three-parameter curve-fitting procedure when data from at least 6 to 10 time points are available.[27] The multipoint approach, first described by Look and Locker,[28] samples the relaxation curve

multiple times after an initial preparation pulse.[29] More recently, the modified Look-Locker (LL) inversion (MOLLI) recovery sequence has been applied to perform in vivo T1 measurements and T1 mapping of the myocardium with high spatial resolution and within a single breath-hold (Figure 6).[30]

The sequence, based on the conventional LL imaging,[28] consists of image acquisitions over different inversion time readouts following a single preparation pulse and permits selective data acquisition and the data merging from multiple LL experiments into one data set. Because T1 mapping methods assume that the voxel consists of a single tissue species (myocardium or blood) and not by a mixture, the most important limitation for clinical application is related to the error due to partial volume contamination from the blood, which can be significant for thin wall structures.[31] From its development, the MOLLI sequence opened a new frontier of clinical applications for myocardial T1 mapping and many variants, based on inversion-recovery, saturation-recovery, or hybrid approaches that are continually developed, to enable faster acquisitions and minimize heart rate dependency, motion, and partial volume effects.[32,33] In particular, the saturation-recovery single-shot acquisition sequence allows a high level of accuracy in T1 measurements performed in phantoms.[34] This sequence stands out clinically, because it has the potential impact to highlight interstitial myocardial fibrosis at an early stage of disease, when it is still reversible.[35]

Figure 6. T1 mapping of the myocardium.

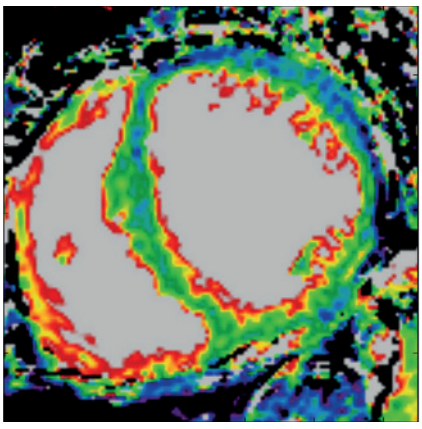

T2 mapping is performed by collecting multiple images with different T2 weighting, achieving multiple points along the T2 decay curve computed using exponential fit.[36] Preliminary T2 mapping methods were based on dark-blood turbo spin-echo sequences and they were very sensitive to motion artifacts and ghosting,[36] although recently, the use of bright-blood T2 prep-based pulse sequences has shown improved performance.[37] The clinical applications of T2 mapping detect edematous myocardial areas in a variety of cardiac pathologies, including acute myocardial infarction, myocarditis, Takotsubo cardiomyopathy, and heart transplant rejection.[38,39] A larger clinical application of T2 mapping can be achieved for determining myocardial viability in cases of acute myocardial edema and for predicting transplant rejection only when dedicated pulse sequences with optimal spatial and temporal resolutions are available.[40] Table 1 provides an overview of the signal intensity of myocardial contents with the different images acquired with CMR.

Magnetic Resonance Spectroscopy

Established Techniques

Human cardiac MRS methods are characterized by technical limitations resulting from the low technique sensitivity, which currently prevents pervasive clinical use. ^{31}P, ^{1}H, ^{13}C, and ^{23}Na are the nuclei studied with MRS. ^{1}H MRS has a higher sensitivity than ^{31}P MRS, so it has a more realistic potential than ^{31}P MRS to become a clinical tool to noninvasively identify viable myocardium with intrinsic contrast. ^{1}H MRS is used for the determination of myocardial fat, carnitine, lactate, myoglobin, and total creatine levels.

Human cardiac MRS methods are characterized by technical limitations resulting from the low technique sensitivity, which currently prevents pervasive clinical use.

The integration of spectroscopy of nuclei other than protons with imaging requires that the magnetic resonance system can operate at two different frequencies. The use of dual-tuned coils, instead of two separated coils, permits clinicians to simplify patient setup and to perform anatomic localization and metabolic data collection in sequence without disturbing and repositioning the patient.

Newly Described Techniques

More recently, ^{13}C and ^{23}Na have achieved more technical relevance due to their potential to characterize myocardial metabolism and viability. Because the natural signal generated by ^{13}C nuclei is very low and difficult to detect with conventional scanners, data acquisition is principally limited by the low natural abundance and the low level of nuclear polarization at thermal equilibrium. However, this obstacle has recently been overcome due to the development of a new technology to enhance the polarization of ^{13}C by a factor of more than 10,000.[41]

Chemical shift imaging (CSI) allows for a higher spatial resolution and the generation of two- or

TABLE 1

Myocardial Tissue Content and Signal Intensity With Different Cardiac Magnetic Resonance Images

Tissue	T1-weighted Images	T2-weighted Images	PD-weighted Images	STIR	Delayed Enhancement
Normal	Isointense	Isointense	Isointense	Isointense	Null
Fibrosis	Isointense	Isointense	Isointense	Moderately hypointense	Hyperintense
Fat	Hyperintense	Isointense	Moderately hyperintense	Null	Markedly hyperintense
Edema	Isointense	Hyperintense	Isointense	Hyperintense	Moderately hyperintense
Hemorrhage	Hypointense	Hypointense	Hypointense	Hypointense	Hypointense

PD, proton density; STIR, short T1 inversion recovery.

three-dimensional maps of metabolite spectra of a given ^{13}C-labeled substrate, in vivo.[42] Some studies in rodents and pigs have shown that CSI is a reliable method to study cardiac metabolism in vivo, by demonstrating the use of hyperpolarized ^{13}C-labeled pyruvate for monitoring the metabolism of lactate, alanine, and bicarbonate over seconds, in both normal and dysfunctional myocardium (Figure 7).[43,44]

Regarding ^{23}Na MRS, even though the nucleus spin quantum number is 3/2, thus providing a strong response to excitation, the sodium sensitivity is only 9.2% of the one achievable for proton. Moreover, sodium concentration within tissues is thousands of times lower than the proton concentration. As a result, the SNR of sodium is 3000 to 20,000 times lower than the SNR of proton.[45] This disadvantage can be partially overcome by using larger voxel sizes, longer acquisition times, and faster pulse sequences—the latter can be used due to the shorter relaxation times of ^{23}Na.[46] Recent studies describe the combination of ^{23}Na magnetic resonance with contrast-enhanced ^{1}H MRI for noninvasively characterizing infarct healing in vivo in dogs and rats, underlying the possibility of achieving even temporal characterization of acute reperfused myocardial infarction.[47]

Figure 7. Hyperpolarized ($^{1\text{-}13}$C) pyruvate map in a pig heart evaluated with chemical shift imaging.

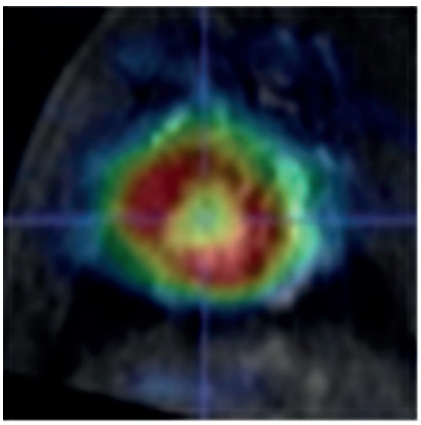

Conclusions

MRI and MRS are noninvasive diagnostic techniques based on the phenomenon of nuclear magnetic resonance. Although MRI uses the signal from protons to produce anatomic images, MRS uses this information to determine metabolite concentration in the tissue examined. This article summarizes the new technical developments in pulse sequences and coils for CMR applications, of which the designs are critical for maximizing data quality and for achieving faster cardiac examination. ■

The authors report no real or apparent conflicts of interest.

References

1. Forder JR, Pohost GM. Cardiovascular nuclear magnetic resonance: basic and clinical applications. *J Clin Invest.* 2003;111:1630-1639.
2. Hoult DI, Richards RE. The signal-to-noise ratio of the nuclear magnetic resonance experiment. 1976. *J Magn Reson.* 2011;213:329-343.
3. Giovannetti G, Hartwig V, Positano V, Vanello N. Radiofrequency coils for magnetic resonance applications: theory, design and evaluation. *Crit Rev Biomed Eng.* 2014;42:109-135.
4. Roemer PB, Edelstein WA, Hayes CE, et al. The NMR phased array. *Magn Reson Med.* 1990;16:192-225.
5. Wintersperger BJ, Reeder SB, Nikolaou K, et al. Cardiac CINE MR imaging with a 32-channel cardiac coil and parallel imaging: impact of acceleration factors on image quality and volumetric accuracy. *J Magn Reson Imaging.* 2006;23:222-227.
6. Friedrich MG. Tissue characterization of acute myocardial infarction and myocarditis by cardiac magnetic resonance. *JACC Cardiovasc Imaging.* 2008;1:652-662.
7. Blamire AM. The technology of MRI—the next 10 years? *Br J Radiol.* 2008;81:601-617.
8. Abdel-Aty H, Simonetti O, Friedrich MG. T2-weighted cardiovascular magnetic resonance imaging. *J Magn Reson Imaging.* 2007;26:452-459.
9. Pettigrew RI, Oshinski JN, Chatzimavroudis G, Dixon WT. MRI techniques for cardiovascular imaging. *J Magn Reson Imaging.* 1999;10:590-601.
10. Doltra A, Stawowy P, Dietrich T, et al. Magnetic resonance imaging of cardiovascular fibrosis and inflammation: from clinical practice to animal studies and back. *Biomed Res Int.* 2013;2013:676489.
11. Mewton N, Liu CY, Croisille P, et al. Assessment of myocardial fibrosis with cardiac magnetic resonance. *J Am Coll Cardiol.* 2011;57:891-903.

12. Anderson LJ, Holden S, Davis B, et al. Cardiovascular T2-star (T2*) magnetic resonance for the early diagnosis of myocardial iron overload. *Eur Heart J*. 2001;22:2171-2179.
13. Ghugre NR, Ramanan V, Pop M, et al. Quantitative tracking of edema, hemorrhage, and microvascular obstruction in subacute myocardial infarction in a porcine model by MRI. *Magn Reson Med*. 2011;66:1129-1141.
14. Westwood MA, Firmin DN, Gildo M, et al. Intercentre reproducibility of magnetic resonance T2* measurements of myocardial iron in thalassaemia. *Int J Cardiovasc Imaging*. 2005;21:531-538.
15. Sarwar A, Shapiro MD, Abbara SR, Cury C. Cardiac magnetic resonance imaging for the evaluation of ventricular function. *Semin Roentgenol*. 2008;43:183-192.
16. Bieri O, Scheffler K. Review fundamentals of balanced steady state free precession MRI. *J Magn Reson Imaging*. 2013;38:2-11.
17. Wintersperger BJ, Nikolaou K, Dietrich O, et al. Single breath-hold real-time cine MR imaging: improved temporal resolution using generalized autocalibrating partially parallel acquisition (GRAPPA) algorithm. *Eur Radiol*. 2003;13:1931-1936.
18. Atkinson DJ, Burstein D, Edelman RR. First-pass cardiac perfusion: evaluation with ultrafast MR imaging. *Radiology*. 1990;174(3 Pt 1):757-762.
19. Wacker CM, Bock M, Hartlep AW, et al. Changes in myocardial oxygenation and perfusion under pharmacological stress with dipyridamole: assessment using T2* and T1 measurements. *Magn Reson Med*. 1999;41;686-695.
20. Manka R, Paetsch I, Schnackenburg B, et al. BOLD cardiovascular magnetic resonance at 3.0 Tesla in myocardial ischemia. *J Cardiovasc Magn Reson*. 2010;12:54.
21. Pruessmann KP, Weiger M, Scheidegger MB, Boesiger P. SENSE: sensitivity encoding for fast MRI. *Magn Reson Med*. 1999;42:952-962.
22. Bydder M, Larkman DJ, Hajnal JV. Generalized SMASH imaging. *Magn Reson Med*. 2002;47:160-170.
23. Griswold MA, Jakob PM, Heidemann RM, et al. Generalized autocalibrating partially parallel acquisitions (GRAPPA). *Magn Reson Med*. 2002;47:1202-1210.
24. Kyriakos WE, Panych LP, Kacher DF, et al. Sensitivity profiles from an array of coils for encoding and reconstruction in parallel (SPACE RIP). *Magn Reson Med*. 2000;44:301-308.
25. Yeh EN, McKenzie CA, Ohliger MA, Sodickson DK. Parallel magnetic resonance imaging with adaptive radius in k-space (PARS): constrained image reconstruction using k-space locality in radiofrequency coil encoded data. *Magn Reson Med*. 2005;53:1383-1392.
26. Santelli C, Schaeffter T, Kozerke S. Radial k-t SPIRiT: autocalibrated parallel imaging for generalized phase-contrast MRI. *Magn Reson Med*. 2014;72:1233-1245.
27. Zhang Y, Yeung HN, O'Donnell M, Carson PL. Determination of sample time for T1 measurement. *J Magn Reson Imaging*. 1998;8:675-681.
28. Look DC, Locker DR. Time saving in measurement of NMR and EPR relaxation times. *Rev Sci Instrum*. 1970;41:250-251.
29. Graumann R, Barfuss H, Hentschel D, Oppelt A. TOMROP: a sequence for determining the longitudinal relaxation time T1 in magnetic resonance tomography [article in German]. *Electromedica*. 1987;55: 67-72.
30. Messroghli DR, Plein S, Higgins DM, et al. Human myocardium: single-breath-hold MR T1 mapping with high spatial resolution-reproducibility study. *Radiology*. 2006;238:1004-1012.
31. Kellman P, Hansen MS. T1-mapping in the heart: accuracy and precision. *J Cardiovasc Magn Reson*. 2014;16:2.
32. Lee JJ, Liu S, Nacif MS, et al. Myocardial T1 and extracellular volume fraction mapping at 3 Tesla. *J Cardiovasc Magn Reson*. 2011;13:75.
33. Xue H, Shah S, Greiser A, et al. Motion correction for myocardial T1 mapping using image registration with synthetic image estimation. *Magn Reson Med*. 2012;67:1644-1655.
34. Chow K, Flewitt JA, Green JD, et al. Saturation recovery single-shot acquisition (SASHA) for myocardial T(1) mapping. *Magn Reson Med*. 2014;71:2082-2095.
35. Barison A, Gargani L, De Marchi D, et al. Early myocardial and skeletal muscle interstitial remodelling in systemic sclerosis: insights from extracellular volume quantification using cardiovascular magnetic resonance. *Eur Heart J Cardiovasc Imaging*. 2015;16:74-80.
36. Salerno M, Kramer CM. Advances in parametric mapping with CMR imaging. *JACC Cardiovasc Imaging*. 2013;6:806-822.
37. Giri S, Chung YC, Merchant A, et al. T2 quantification for improved detection of myocardial edema. *J Cardiovasc Magn Reson*. 2009;11:56.
38. Ferreira VM, Piechnik SK, Robson MD, et al. Myocardial tissue characterization by magnetic resonance imaging: novel applications of T1 and T2 mapping. *J Thorac Imaging*. 2014;29:147-154.
39. Thavendiranathan P, Walls M, Giri S, et al. Improved detection of myocardial involvement in acute inflammatory cardiomyopathies using T2 mapping. *Circ Cardiovasc Imaging*. 2012;5:102-110.
40. Usman AA, Taimen K, Wasielewski M, et al. Cardiac magnetic resonance T2 mapping in the monitoring and follow-up of acute cardiac transplant rejection: a pilot study. *Circ Cardiovasc Imaging*. 2012;5: 782-790.
41. Ardenkjaer-Larsen JH, Fridlund B, Gram A, et al. Increase in signal-to-noise ratio of >10,000 times in liquidstate NMR. *Proc Natl Acad Sci U S A*. 2003;100:10158-10163.
42. Klose U, Jiru F. Principles of MR spectroscopy and chemical shift imaging. In: Landini L, Positano V, Santarelli MF, eds. *Advanced Image Processing in Magnetic Resonance Imaging*. Boca Raton, FL: Taylor & Francis Group; 2005:369-410.
43. Merritt ME, Harrison C, Storey C, et al. Hyperpolarized ^{13}C allows a direct measure of flux through a single enzyme-catalyzed step by NMR. *Proc Natl Acad Sci U S A*. 2007;104:19773-19777.
44. Schroeder MA, Cochlin LE, Heather LC, et al. In vivo assessment of pyruvate dehydrogenase flux in the heart using hyperpolarized carbon-13 magnetic resonance. *Proc Natl Acad Sci U S A*. 2008;105: 12051-12056.
45. Madelin G, Regatte RR. Biomedical applications of sodium MRI in vivo. *J Magn Reson Imaging*. 2013;38:511-529.
46. Jansen MA, Van Emous JG, Nederhoff MGJ, Van Echteld CJ. Assessment of myocardial viability by intracellular ^{23}Na magnetic resonance imaging. *Circulation*. 2004;110:3457-3464.
47. Hillenbrand HB, Becker LC, Kharrazian R, et al. ^{23}Na MRI combined with contrast-enhanced ^{1}H MRI provides in vivo characterization of infarct healing. *Magn Reson Med*. 2005;53: 843-850.

MAIN POINTS

- Cardiac magnetic resonance (CMR) is a relevant diagnostic tool for the evaluation of cardiac disease due to its noninvasive nature, the absence of ionizing radiation, the three-dimensional visualization of the heart chambers, the high image quality, and its good temporal resolution.
- Since the development of phased-array coils, magnetic resonance vendors introduced multiple receiver channel systems to take advantage of the improved sensitivity and extended field of view provided by multiple coil design.
- Spin echo sequences are used for anatomic imaging and tissue characterization, whereas gradient echo sequences are used for acquiring cine images to calculate volumes and to assess regional and global cardiac function in both the right and left ventricles.
- The inversion-recovery gradient-echo sequence provides high contrast between normal myocardium and scarring by nulling the signal from normal myocardium. This sequence is largely used in the clinical setting to assess the presence of fibrosis within the myocardium.
- Tissue characterization through assessing myocardial T1 and T2 mapping and spectroscopy currently represent the two primary fields of CMR development. The measurement of T1 and T2 mapping aims to detect early myocardial degenerative and infiltrative diseases, whereas spectroscopy aims to assess myocardial metabolism.